25. The experimental rate constants and activation energies can be used to obtain a minimum H_{ab} value (*16*). With a density of states of 0.3 eV^{-1} per gold atom, a reorganization energy of 0.9 eV, and a rate constant of 3×10^6 s^{-1}, nonadiabatic electrochemical Marcus theory gives a minimum H_{ab} value of 52 cm^{-1} at 298 K. The calculated H_{ab} in the case of the $n = 4$ model compound was 2.6 cm^{-1}. Calculated H_{ab} values cannot be directly compared with experimental H_{ab} values because the model system has a ferrocene group where the experimental system has gold atoms. To account for this difference, we assume tight coupling between the bridge and one carbon atom of the ferrocene in the model system and tight coupling between the bridge and one gold atom in the experimental system. Additionally, we assume that the additional vinylene in the model system is equivalent to the methyl thiol in the experimental system. The quantum calculation gives a wave function amplitude on the ferrocenyl carbon of 0.14. Division of the calculated H_{ab} by this coefficient yields a more appropriate value of 18 cm^{-1} for comparison with the lower limit of the experimental H_{ab} value. This value is within a factor of 3 of the minimum obtained from experiment. Given the uncertainties in the calculation, we consider this result consistent with the conclusion that the rate is not limited by the electronic coupling.
26. L. D. Zusman, *Chem. Phys.* **49**, 295 (1980).
27. J. Barthel, K. Bachhuber, R. Buchner, H. Hetzenauer, *Chem. Phys. Lett.* **165**, 369 (1990). $\tau_L = (\varepsilon_\infty/\varepsilon_o)\tau_D$, where τ_L is the longitudinal polarization time, ε_∞ is the infinite-frequency dielectric constant, ε_o is the static dielectric constant, and τ_D is the Debye relaxation time.
28. G. K. Rowe, S. E. Creager, *Langmuir* **7**, 2307 (1991).
29. H.D.S. acknowledges an NSF Graduate Fellowship. S.P.D. acknowledges support from National Research Service Award 5 T32 GM08412 from the National Institute of General Medical Science. H.D.S., S.P.D., and C.E.D.C. acknowledge support from the NSF (CHE-9412720) and the Stanford Office of Technology Licensing. J.F.S., A.R.C., M.D.N., and S.W.F. acknowledge support from the Chemical Sciences Division, Department of Energy (DE-AC02-98CH10886).

13 September 2000; accepted 17 January 2001

Automated Solid-Phase Synthesis of Oligosaccharides

Obadiah J. Plante, Emma R. Palmacci, Peter H. Seeberger*

Traditionally, access to structurally defined complex carbohydrates has been very laborious. Although recent advancements in solid-phase synthesis have made the construction of complex oligosaccharides less tedious, a high level of technical expertise is still necessary to obtain the desired structures. We describe the automated chemical synthesis of several oligosaccharides on a solid-phase synthesizer. A branched dodecasaccharide was synthesized through the use of glycosyl phosphate building blocks and an octenediol functionalized resin. The target oligosaccharide was readily obtained after cleavage from the solid support. Access to certain complex oligosaccharides now has become feasible in a fashion much like the construction of oligopeptides and oligonucleotides.

The understanding of oligosaccharides and glycoconjugates in nature is still in its infancy (*1*). Cell surface glycoconjugates are involved in signal transduction pathways and cellular recognition processes and have been implicated in many disease states (*2*). A major impediment to the rapidly growing field of molecular glycobiology is the lack of pure, structurally defined carbohydrates and glycoconjugates. These biomolecules are often found in low concentrations and in microheterogeneous form in nature, greatly complicating their identification and isolation. The procurement of sufficient quantities of defined oligosaccharides required for detailed biophysical and biochemical studies therefore relies on efficient synthetic methods.

Although much progress has been made in oligosaccharide synthesis (*3*), the construction of complex carbohydrates remains time consuming and is carried out by a small number of specialized laboratories. The necessary functionalization of all hydroxyl groups present on a monosaccharide is one of the main challenges in oligosaccharide construction. The development of a protecting group scheme that allows for the manipulation of individual hydroxyl groups is pivotal for the success of the synthetic route. Permanent protecting groups, such as benzyl ethers, are installed at positions where a free hydroxyl will be present in the final deprotected molecule. Temporary protecting groups, such as esters, are used to mask hydroxyls that will be exposed at a certain stage of the synthesis. The liberated hydroxyl group then serves as a nucleophile in the reaction with a glycosylating agent.

The stereospecific formation of glycosidic bonds is the central challenge in carbohydrate chemistry (Fig. 1). The chemical formation of a glycosidic linkage involves activation of a glycosyl donor to create a reactive electrophilic species that couples with a nucleophilic acceptor hydroxyl. This coupling reaction can take two possible pathways resulting in formation of either α- or β-anomers. Current methods to control the stereochemistry of the anomeric center rely on the participation of a neighboring functionality, such as an ester-protecting group on the C2 hydroxyl. Formation of a cyclic oxonium ion intermediate shields one face of the molecule, leading exclusively to the formation of trans-glycosidic linkages. Cis-glycosidic bonds are difficult to construct with high specificity because neighboring group participation is not possible.

Department of Chemistry, Massachusetts Institute of Technology, Cambridge, MA 02139, USA.

*To whom correspondence should be addressed. E-mail: seeberg@mit.edu

The evolution of a solid-phase paradigm for the construction of oligosaccharides was initiated with Frechet's synthesis of di- and trisaccharides on a polymer support in 1971 (*4*). Since then, solid-phase oligosaccharide synthesis has seen many advancements. Various glycosyl donors, such as anomeric sulfoxides (*5*) and anhydrosugars (*5*), have been applied to the synthesis of carbohydrates on a polymer support. Several linkers serving to connect the growing oligosaccharide chain to the polymer support have been introduced with different reactivities and cleavage procedures (*6*). Notably, a combinatorial split-and-mix approach on a support resulted in the synthesis of a library of *N*-acylated di- and trisaccharides (*7*). Although advancements in solid-phase chemistry have allowed for the construction of complex molecules, the manipulations remain tedious and time consuming.

Ultimately, a general, automated method for oligosaccharide assembly will allow for the rapid preparation of structures of interest. Oligonucleotides (*8*) and oligopeptides (*9*) are now routinely prepared in an efficient manner on automated synthesizers with solid-phase strategies. The solid-phase paradigm lends itself particularly well to automation of oligosaccharide synthesis as the repetitive nature of glycosylation and deprotection can easily be framed into a coupling cycle. Excess reagents can be used to drive reactions to completion, and resin washes can remove any soluble impurities. Only a single purification step is necessary after the sugar is liberated from the solid support.

Mindful of the advantages of solid-support synthesis, we considered several key issues for the development of an automated oligosaccharide synthesizer: (i) an instrument capable of performing repetitive chemical manipulations at variable temperatures, (ii) the design of an overall synthetic strategy with either the reducing or the nonreducing end of the growing carbohydrate chain attached to the support (*10*), (iii) selection of a polymer and linker that are inert to all reaction conditions during the synthesis but cleaved efficiently when desired, (iv) protecting group strategies consistent with the complexity of the target oligosaccharide, and (v)

stereospecific and high yielding glycosylation reactions.

Rather than designing a new machine, we opted to reengineer an existing apparatus used in automated peptide synthesis (*11*). Several adaptations were necessary before the peptide synthesizer could be used for carbohydrate synthesis (*12*). Using this modified peptide synthesizer, we undertook a systematic investigation of the variables involved in automated solid-phase oligosaccharide synthesis. We chose the "acceptor bound" strategy for solid-phase oligosaccharide synthesis (*13*). In this method, the reactive glycosylating agent is delivered in solution while the nucleophilic acceptor hydroxyl group is exposed on the solid support. Productive coupling events result in support-bound oligosaccharides that are purified by simply washing the soluble side products through a filter. Removal of a temporary protecting group on the newly formed saccharide unit reveals another hydroxyl group, thereby continuing the coupling cycle.

To explore the compatibility of glycosylating agents and protecting groups with a solid-phase linker and a polymer support, we investigated the construction of polymannosides. The synthesis of α-mannosides has been the focus of substantial research because of their occurrence in biological structures such as glycolipids and *N*-linked glycoproteins (*14*, *15*). A series of α-(1→2) mannosides (Scheme 1, **3** to **5**) served as our initial targets for automation because structures of this type have been synthesized previously in solution and on the solid support (*16*). Trichloroacetimidate donor **2** was chosen as the donor building block because it can be prepared on a multigram scale, is activated at room temperature, and bears a C2-ester functionality to control the anomeric configuration of the polymer (*17*). Activation of **2** was carried out under acidic conditions with the Lewis acid trimethylsilyl trifluoromethanesulfonate (TMSOTf). Removal of the acetyl ester-protecting group was accomplished under basic conditions with sodium methoxide.

To allow for the use of acidic and basic reaction conditions in the coupling cycle, we investigated a polymer support and linker for compatibility (*18*). A variety of commercially available polymer supports were examined. Merrifield's resin (1% cross-linked polystyrene) and polystyrene-based Argopore displayed excellent properties throughout the coupling cycle. Our previous work demonstrated that olefinic linker **1** was stable to the coupling cycle conditions while readily cleaved from the solid support at the end of the synthesis by olefin cross metathesis. By varying the concentration and quantity of reagents as well as the reaction times, we arrived at the cycle shown in Table 1. Applying the conditions in Table 1 with octenediol functionalized 1% cross-linked polystyrene, the synthesis of pentamannoside **3** was carried out in 14 hours (Scheme 1).

Analysis of the resin-bound oligosaccharide is essential for the successful development of a solid-phase synthesis method (*19*). Two-dimensional nuclear magnetic resonance (2D-NMR) analysis of the resin-bound pentamer **6** was performed with high-resolution magic angle spinning (HR-MAS) NMR techniques (Fig. 2). Analysis of the NMR spectra revealed characteristic anomeric signals between 97 and 103 parts per million. Further homonuclear total correlation spectroscopy (TOCSY) HR-MAS analysis confirmed the presence of five unique anomeric protons (*20*). In accordance with previous experiments, minor line broadening was observed in the spectra of the resin-bound sample (*21*). Overall, the HR-MAS NMR data of the polymer-bound pentamer corresponded unequivocally with an authentic pentamer sample prepared in solution. The remarkable purity of the resin-bound pentasaccharide **6**, after nine synthetic steps without any purification, encouraged us to explore the synthesis of larger structures. Heptamer **4** and decamer **5** were prepared in average yields of 90 to 95% per step. The short reaction times, 3 hours per monomer unit, allowed for the synthesis of **4** in 20 hours and 42% overall yield. As a comparison, we manually synthesized heptamannoside **4** on the solid support in 14 days and 9% overall yield (*18*). These results demonstrate that the synthesis of a linear oligosaccharide is fast and high yielding when constructed on an automated synthesizer.

Given the success with the automated α-mannoside construction, the fully protected phytoalexin elicitor (PE) β-glucan **7** was selected as a more complex target structure (Fig. 3) (*22*). The presence of a fungal β-glucan oligosaccharide triggers the soybean plant to release antibiotic phytoalexins. The response initiated by the PE β-glucans in the

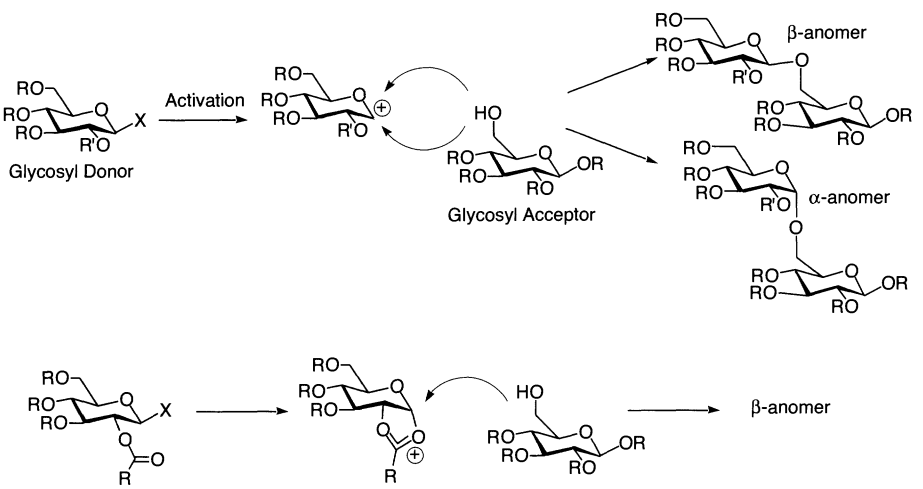

Fig. 1. Stereochemical issues in the synthesis of carbohydrates: Oligosaccharides require the formation of a particular stereoisomer (α or β anomer) during each coupling event. The use of participating groups, such as esters, leads to exclusive formation of trans-glycosidic linkages.

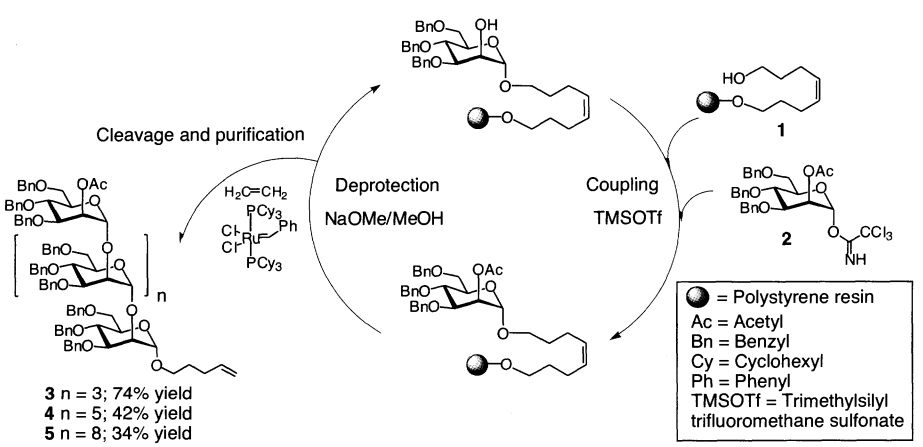

Scheme 1. Automated oligosaccharide synthesis with trichloroacetimidates. Glycosylation conditions: 25-μmol scale: 25 μmol of resin (83 mg, 0.30 mmol/g loading); 10 equiv. donor **2** (160 mg); 0.5 equiv. TMSOTf (1 ml, 0.0125 M TMSOTf in CH_2Cl_2) repeated two times for 30 min each. Deprotection conditions: 25-μmol scale: 10 equiv. NaOMe (0.5 ml, 0.5 M NaOMe in MeOH) in 5 ml of CH_2Cl_2 repeated two times for 30 min each.

host soybean plant is the most studied defense mechanism in plants. These oligosaccharides have been synthesized previously in solution (*23*) and on the solid support (*24*) and were expected to serve well as a benchmark in our automation endeavor.

For the synthesis of the branched β-(1→3)/β-(1→6) PE structure, we envisioned the use of two different glycosyl phosphate donors, **8** and **9**. Recently, we introduced glycosyl phosphates as glycosylating agents that are readily prepared from glycal precursors and that performed well in solution and on a solid support (*25*). Strategic protecting group considerations prompted us to use the levulinoyl ester as a 6-*O* temporary protecting group and the 2-*O*-pivaloyl group to ensure complete β-selectivity in the glycosylation reaction. Deprotection of the levulinoyl ester was accomplished with a hydrazine solution in pyridine/acetic acid, whereas the phosphate building block was activated with TMSOTf.

Unlike peptide and nucleic acid synthesis, many of the manipulations involved in oligosaccharide chemistry are not carried out at room temperature. Drawing from solution-phase studies, we were cognizant that the use of glycosyl phosphates, like many donors (*26*), would require low temperature for optimal results. To address this need, we designed a temperature-controlled reaction vessel. The vessel is enclosed by a cooling jacket that is easily attached to a commercial cooling apparatus. Model reactions with phosphate donor **8** demonstrated the ease of incorporating a temperature variable in the automation cycle.

The coupling and deprotection conditions were adjusted for the use of glycosyl phosphates and levulinoyl esters, resulting in the cycle shown in Table 1 (phosphate cycle). The activation of phosphate donor **8** at −15°C required shorter reaction times than were needed for trichloroacetimidate **2**, as determined in preliminary solution-phase studies. As anticipated from previous studies (*27*), the levulinate ester could be rapidly removed at +15°C (15 min), compared with longer reaction times necessary for acetyl ester cleavage. The levulinoyl group deprotection cycle incorporates a different washing cycle (pyridine/acetic acid) than the acetyl group to ensure removal of any excess hydrazine. As in the synthesis of polymannosides **3** to **5**, double glycosylations and double deprotections were used. Incorporation of these modifications to the automated cycle resulted in an excellent yield [92% by high-pressure liquid chromatography (HPLC) analysis] of a model β-(1→6) trisaccharide.

The automated cycle was then applied to the synthesis of more complex PE oligosaccharides with alternating phosphate building blocks (Scheme 2). Branched hexasaccharide **10** was constructed in 10 hours in >80% yield as judged by HPLC analysis. Also, we prepared dodecasaccharide **7** (Fig. 3) in 17 hours and >50% yield using the same cycle. Notably, the solution-phase synthesis of only two phosphate building blocks was necessary, which greatly reduces the manual labor usually required to assemble a structure of this size. The expedient generation of material through automation represents a major improvement over conventional methods for polysaccharide synthesis.

We have demonstrated that both glycosyl phosphates and trichloroacetimidates are useful donors in the automated synthesis of oligosaccharides, as well as the utility of acetate and levulinate esters as temporary protecting groups. To illustrate the generality of this method, we synthesized trisaccharide **13**, incorporating all aspects of our automated chemistry. This trisaccharide motif occurs in complex type *N*-linked glycoprotein structures and contains two challenging linkages. Glycosylations of the C2 position of mannose with glucosamine donors and the C4 hydroxyl of glucosamine with galactose donors are notoriously difficult reactions, often leading to the formation of unwanted side products (*28*).

Table 1. Cycles used with trichloroacetimidate and phosphate donors.

Step	Function	Reagent	Time (min)
		Trichloroacetimidate cycle	
1	Couple	10 equiv. donor and 0.5 equiv. TMSOTf	30
2	Wash	Dichloromethane	6
3	Couple	10 equiv. donor and 0.5 equiv. TMSOTf	30
4	Wash	Dichloromethane	6
5	Wash	1:9 methanol:dichloromethane	6
6	Deprotection	2 × 10 equiv. NaOMe (1:9 methanol:dichloromethane)	60
7	Wash	1:9 methanol:dichloromethane	4
8	Wash	0.2 M acetic acid in tetrahydrofuran	4
9	Wash	Tetrahydrofuran	4
10	Wash	Dichloromethane	6
		Phosphate cycle	
1	Couple	5 equiv. donor and 5 equiv. TMSOTf	30
2	Wash	Dichloromethane	6
3	Couple	5 equiv. donor and 5 equiv. TMSOTf	30
4	Wash	1:9 methanol:dichloromethane	4
5	Wash	Tetrahydrofuran	4
6	Wash	3:2 pyridine:acetic acid	3
7	Deprotection	2 × 20 equiv. hydrazine (3:2 pyridine:acetic acid)	30
8	Wash	3:2 pyridine:acetic acid	3
9	Wash	1:9 methanol:dichloromethane	4
10	Wash	0.2 M acetic acid in tetrahydrofuran	4
11	Wash	Tetrahydrofuran	4
12	Wash	Dichloromethane	6

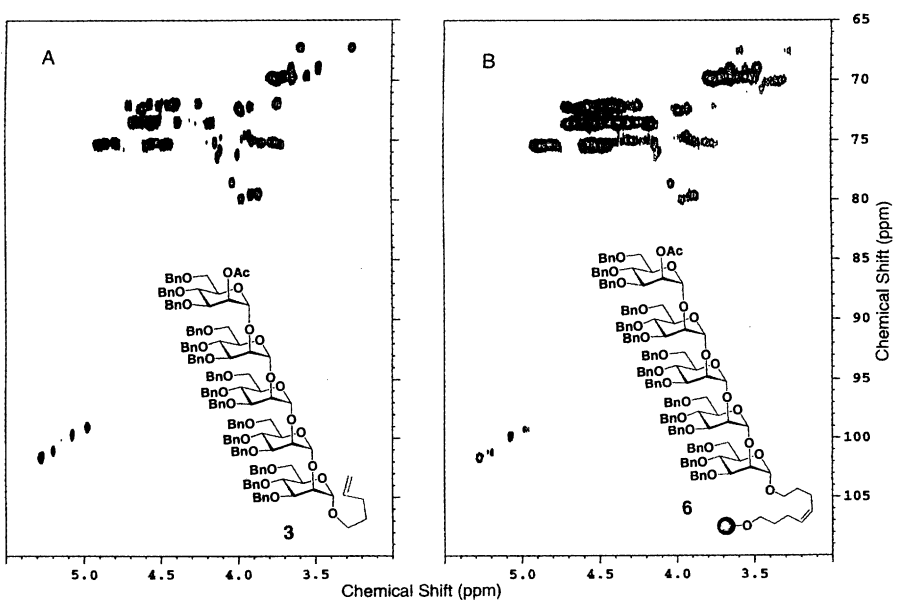

Fig. 2. 2D-NMR comparison of **(A)** solution-phase and **(B)** resin-bound pentamer.

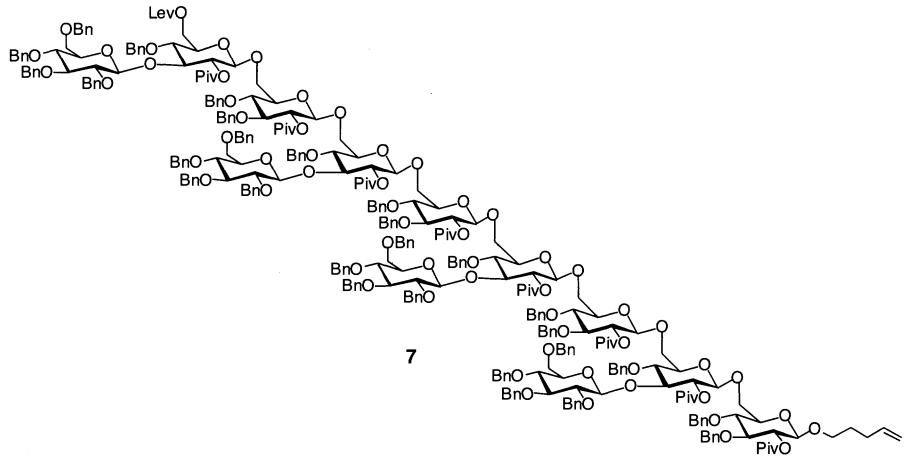

Fig. 3. Dodecamer phytoalexin elicitor β-glucan.

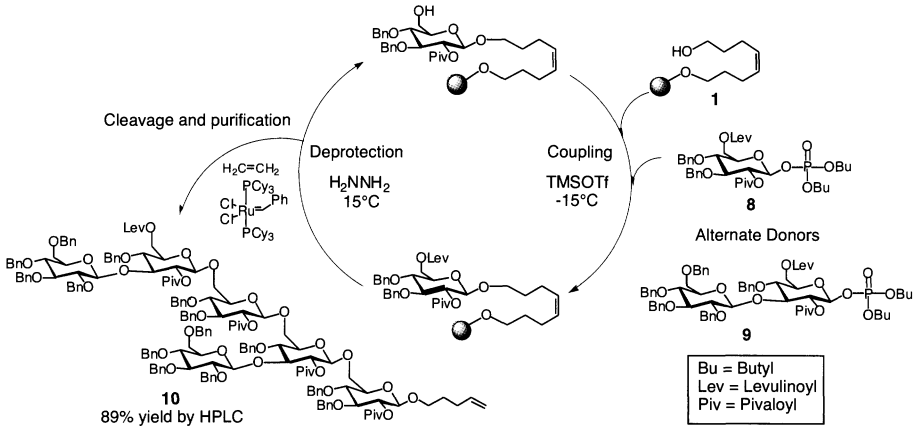

Scheme 2. Automated oligosaccharide synthesis with glycosyl phosphates. Glycosylation conditions: 25 μmol scale: 25 μmol resin (83 mg, 0.30 mmol/g loading); 5 equiv. donor **8** or **9** (90 and 170 mg, respectively); 5 equiv. TMSOTf (1 ml, 0.125 M TMSOTf in CH_2Cl_2) repeated two times for 15 min each at –15°C. Deprotection conditions: 25 μmol scale: 4 ml, 0.25 M N_2H_4 in pyridine:acetic acid (3:2) repeated two times for 15 min each at 15°C.

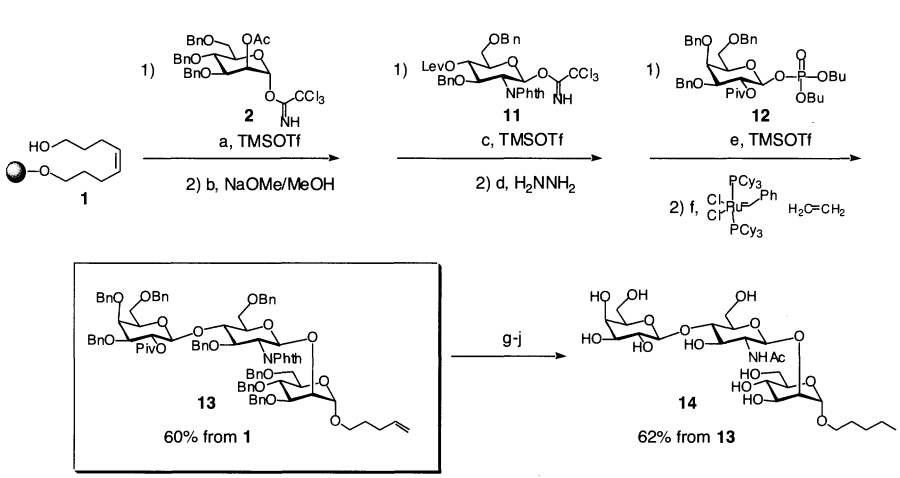

Scheme 3. Automated synthesis of trisaccharide **13**. 100 μmol scale: 100 μmol resin (333 mg, 0.30 mmol/g loading); a, 4 equiv. donor **2**, 0.4 equiv. TMSOTf repeated two times for 30 min each. b, 5 equiv. NaOMe in CH_2Cl_2 repeated two times for 30 min each. c, 4 equiv. donor **11**, 0.4 equiv. TMSOTf repeated two times for 15 min each at –15°C. d, 4 ml, 0.25 M N_2H_4 in pyridine:acetic acid (3:2) repeated two times for 15 min each at 15°C. e, 4 equiv. donor **12**, 4 equiv. TMSOTf repeated two times for 15 min each at –15°C. f, 16.4 mg catalyst, 1 atm CH_2CH_2, CH_2Cl_2. g, N_2H_4, EtOH, 90°C. h, Ac_2O, MeOH/CH_2Cl_2. i, LiOH, THF/CH_3OH. j, H_2, Pd/C, EtOH.

The automated synthesis of trisaccharide **13** required the preparation monosaccharide building blocks (**2**, **11**, and **12**). Donor **2** was chosen on the basis of the glycosylation and deprotection protocols developed for the synthesis of α-(1→2) mannosides. Glucosamine donor **11** was designed with the phthalimide amine-protecting group to confer β-selectivity during glycosylation. Incorporation of a levulinate ester at the C4 position of **11** allows for rapid deprotection with hydrazine as demonstrated in the synthesis of the PE β-glucans. Galactosyl phosphate **12** was chosen to fashion the terminal glycosidic linkage on the basis of the high reactivity of this donor with unreactive substrates (*25*).

The automated synthesis of trisaccharide **13** was carried out with the cycle described in Scheme 3 (*29*). HPLC analysis of the crude reaction mixture after cleavage from the support indicated a 60% overall yield. Subsequent removal of all protecting groups was carried out to demonstrate that oligosaccharides prepared in an automated fashion are efficiently deprotected. Cleavage of the phthalimide group with hydrazine (*30*) and *N*-acetylation with acetic anhydride were followed by removal of the pivaloyl group with LiOH (*5*). Global debenzylation proceeded smoothly with concomitant reduction of the olefin functionality to afford *n*-pentyl glycoside **14** in 62% yield from the fully protected trimer **13**. The cleavage conditions described here for the removal of phthaloyl, pivaloyl, and benzyl groups are routine procedures (*31*) that can be applied to a wide variety of substrates.

In summary, these examples illustrate major improvements in time and yield as compared with manual syntheses of oligosaccharides. A glycosylation/deprotection cycle was developed and applied to the synthesis of a decamer of an α-(1→2) mannoside. Two phytoalexin elicitor β-glucans, hexasaccharide **10** and dodecasaccharide **7**, were constructed in rapid fashion with glycosyl phosphates. Trisaccharide **13** was assembled with both glycosyl phosphate and trichloroacetimidate donors and a protecting group strategy based on acetate and levulinate esters. The automated method described above represents an important advance toward streamlining the synthesis of oligosaccharides.

Although several limitations still exist in oligosaccharide construction, it is now possible to transfer many solution and solid-phase chemistries to an automated synthesizer. A number of challenges such as the synthesis of sialic acid containing oligosaccharides and heparinlike glycosaminoglycans still remain. Additional research in these areas is needed to further advance the field of oligosaccharide synthesis. The ease of acquiring defined structures from a machine will impact the field of glycobiology such that we may one day be able to fully

appreciate the importance of oligosaccharides and glycoconjugates in nature.

References and Notes

1. R. A. Dwek, *Chem. Rev.* **96**, 683 (1996).
2. S. Hakomori, *Adv. Cancer Res.* **52**, 257 (1989).
3. G. J. Boons, Ed., *Carbohydrate Chemistry* (Blackie, London, 1998).
4. J. M. J. Frechet, C. Schuerch, *J. Am. Chem. Soc.* **93**, 492 (1971).
5. S. J. Danishefsky *et al.*, *Science* **260**, 1307 (1993).
6. P. H. Seeberger, W.-C. Haase, *Chem. Rev.* **100**, 4349 (2000).
7. R. Liang *et al.*, *Science* **274**, 1520 (1996).
8. M. H. Caruthers, *Science* **230**, 281 (1985).
9. E. Atherton, R. C. Sheppard, *Solid-Phase Peptide Synthesis: A Practical Approach* (Oxford Univ. Press, Oxford, UK, 1989).
10. Y. Ito, S. Manabe, *Curr. Opin. Chem. Biol.* **2**, 701 (1998).
11. Applied Biosystems Inc. Model 433A peptide synthesizer.
12. The machine was equipped with seven reagent bottles, four for washing and three for glycosylation and deprotection reagents. Small cartridges containing the donor species were loaded into the synthesizer manually before the synthesis. A cycle was programmed to operate all steps without any operator intervention. The machine controlled the delivery of all reagents and donor species to the reaction vessel and the mixing of the contents of the vessel.
13. B. Merrifield, *J. Am. Chem. Soc.* **85**, 2149 (1963).
14. M. A. J. Ferfuson, A. F. Williams, *Annu. Rev. Biochem.* **57**, 285 (1988).
15. R. Kornfeld, S. Kornfeld, *Annu. Rev. Biochem.* **54**, 631 (1985).
16. S. P. Douglas, D. M. Whitfield, J. J. Krepinsky, *J. Am. Chem. Soc.* **117**, 2116 (1995).
17. J. Rademann, R. R. Schmidt, *J. Org. Chem.* **62**, 3989 (1997), and references therein.
18. R. B. Andrade *et al.*, *Org. Lett.* **1**, 1811 (1999).
19. B. Yan, *Acc. Chem. Res.* **31**, 621 (1998).
20. For on-resin TOCSY analysis of **6**, see supporting data available on *Science* Online (*32*).
21. P. H. Seeberger *et al.*, *Angew. Chem. Int. Ed. Engl.* **36**, 491 (1997).
22. A. Darvill *et al.*, *Glycobiology* **2**, 181 (1992).
23. P. Fugedi *et al.*, *Carbohydr. Res.* **164**, 297 (1987).
24. K. C. Nicolaou *et al.*, *J. Am. Chem. Soc.* **119**, 449 (1997), and references therein.
25. O. J. Plante *et al.*, *Org. Lett.* **1**, 211 (1999).
26. D. Kahne *et al.*, *J. Am. Chem. Soc.* **111**, 6811 (1989).
27. N. M. Spijker, P. Westerduin, C. A. A. van Boeckel, *Tetrahedron* **48**, 6297 (1992).
28. H. Lonn, *Carbohydr. Res.* **139**, 105 (1985).
29. For a detailed description of the coupling cycle used, see the table in the supplemental information (*32*).
30. D. Bundle, S. Josephson, *Can. J. Chem.* **57**, 662 (1979).
31. P. P. Deshpande, S. J. Danishefsky, *Nature* **387**, 164 (1997).
32. Supplementary material is available at www.sciencemag.org/cgi/content/full/1057324/DC1.

33. Financial support from the American Chemical Society (ACS) Division of Organic Chemistry (Pfizer Graduate Fellowship for O.J.P.), the NIH Biotechnology Training Grant (fellowship for O.J.P.), and Merck (fellowship for E.R.P.) and partial funding from the ACS Petroleum Research Fund (ACS-PRF 34649-G1) and the Mizutani Foundation for Glycoscience are gratefully acknowledged. Funding for the MIT-DCIF Inova 501 was provided by NSF (award CHE-9808061) and the NMR facility at the Francis Bitter Magnet Laboratory was provided by the NIH (Grant RR-00995). We thank S. J. Lippard and J. Stubbe for their thoughtful discussion of this manuscript, S. S. Pochapsky for recording the HR-MAS NMR, and D. M. Ratner for assistance in modifying peptide synthesizers.

9 November 2000; accepted 23 January 2001
Published online 1 February 2001;
10.1126/science.1057324
Include this information when citing this paper.

Redox State of Mars' Upper Mantle and Crust from Eu Anomalies in Shergottite Pyroxenes

M. Wadhwa

The oxidation state of basaltic martian meteorites is determined from the partitioning of europium (Eu) in their pyroxenes. The estimated redox conditions for these samples correlate with their initial neodymium and strontium isotopic compositions. This is interpreted to imply varying degrees of interaction between the basaltic parent melts, derived from a source in the martian mantle, and a crustal component. Thus, the mantle source of these martian basalts may have a redox state close to that of the iron-wüstite buffer, whereas the martian crust may be more oxidized (with a redox state higher than or equal to that of the quartz-fayalite-magnetite buffer). A difference in redox state of more than 3 log units between mantle and crustal reservoirs on Mars could result from oxidation of the crust by a process such as aqueous alteration, together with a subsequent lack of recycling of this oxidized crust through the reduced upper mantle.

Determination of the redox state of Mars' mantle and crust would help to estimate elemental distributions between these silicate reservoirs and the core, thereby leading to a better understanding of the accretion and differentiation history of the planet. The red color of the martian surface is attributed to the presence of ferric minerals in the weathered, highly oxidized regolith (*1*). The silicate interior (that is, the mantle and crust) may be less oxidized than the regolith, but there are no direct estimates of its redox state. Indirect estimates of the oxidation state of the martian interior are mostly based on model compositions (specifically, FeO content) of the bulk silicate portion of Mars (BSM). Some of these compositions are derived from cosmochemical models with adjustable parameters fit to density distribution estimates from geophysical data (*2–6*). Others are from the bulk compositions of martian meteorites (*7–9*), which are currently the only samples of the crust of Mars available for study (*10*). A general feature of these models has been the prediction of FeO enrichment in the BSM relative to Earth's mantle, attributed to relatively oxidizing conditions on Mars.

Attempts to obtain estimates of redox conditions on Mars have also been made from the compositions of Fe-bearing minerals in the shergottites, a class of martian meteorites composed of basaltic and lherzolitic rocks, parent magmas of which are thought to represent fractionated partial melts of the martian mantle (*10*). Most of these studies rely on the compositions of coexisting Fe-Ti oxides (*11–14*) and indicate a range of oxidation conditions. However, because these oxides are among the very last phases to crystallize and are susceptible to subsolidus reequilibration, they may not record primary magmatic redox conditions. One investigation based on stoichiometric calculations of Fe^{3+}/Fe^{2+} in shergottite pyroxenes suggested that their source region in the martian mantle may be substantially reduced (*15*). However, a subsequent study (*16*) pointed out large uncertainties in the approach taken by (*15*). Therefore, the issue of the redox state of Mars' silicate interior has so far remained contentious.

Here, magmatic oxidation conditions for the basaltic shergottites were determined from the partitioning of Eu in the earliest crystallizing minerals. Eu is the only rare earth element (REE) than can exist in the divalent and trivalent states under magmatic conditions (other REEs are trivalent). The Eu mineral/melt distribution coefficient (D_{Eu}) for a particular mineral is dependent on the Eu^{3+}/Eu^{2+} ratio in the magma, which in turn is predominantly a function of the prevailing redox condition during crystallization (*17*). Partitioning experiments for synthetic high-Ca pyroxene (augite) and plagioclase with compositions similar to those in the angrites (a class of basaltic meteorites) have established the relation between D_{Eu}/D_{Gd} for these minerals (used as a proxy for the Eu^{3+}/Eu^{2+} ratio in the melt) and oxygen fugacity (f_{O_2}) (*18*). Although analogous experiments (that is, over a wide range of f_{O_2} conditions) have not been performed for the basaltic shergottites, the relation between D_{Eu}/D_{Gd} and f_{O_2} for shergottite minerals may be similar to that for angrite minerals because $(D_{Eu}/D_{Gd})_{augite}$ values from a set of experiments on a shergottite analog composition (*19*, *20*) fall on the same curve as that defined by the data from

Department of Geology, The Field Museum, 1400 South Lake Shore Drive, Chicago, IL 60605, USA. E-mail: mwadhwa@fieldmuseum.org